Food Chemistry: X 16 (2022) 100498

Contents lists available at ScienceDirect

Food Chemistry: X

journal homepage: www.sciencedirect.com/journal/food-chemistry-x

Differences between water-soluble and water-insoluble melanin derived from *Inonotus hispidus* mushroom

Xiaomin Li [a,b], Wenya Wu [a,b], Fengpei Zhang [a,b], Xin Hu [a,b], Yuan Yuan [a,b], Xiaoping Wu [a,b], Junsheng Fu [a,b,*]

[a] College of Life Sciences, Fujian Agriculture and Forestry University, Fuzhou, Fujian 350002, China
[b] Mycological Research Center, Fujian Agriculture and Forestry University, Fuzhou, Fujian 350002, China

ARTICLE INFO

Keywords:
Inonotus hispidus
Melanin
Structural characterization
Antioxidant activity

ABSTRACT

Melanin is a natural pigment with a high content and a complex polymer structure. In this study, both water-soluble and water-insoluble melanin were obtained from the fruiting bodies of the mushroom *Inonotus hispidus*, and scanning electron microscopy (SEM), ultraviolet (UV) absorption, Fourier transform infrared (FTIR) spectroscopy, elemental analysis, nuclear magnetic resonance (NMR) spectroscopy, pyrolysis gas chromatography mass spectroscopy (Py-GCMS), and matrix-assisted laser desorption/ionization-time of flight mass spectrometry (MALDI-TOF-MS/MS) were used to analyze the water-soluble and water-insoluble *I. hispidus* fungal melanin (IHFM). Differences in the chemical composition and structure of *I. hispidus* fungal melanin (IHFM) were found. Studies showed that both have a maximum absorbance at 226 nm, and the maximum mass-to-charge ratios are $[M + H]^+$ m/z = 272.2434 and 272.0308, respectively. Elemental analysis revealed that they both contain C, H, N, O, and do not contain sulfur, which is only found in eumelanin. The differences between water-soluble and water-insoluble IHFM may relate to the following factors: (i) the microscopic particles of water-soluble IHFM are relatively small, the arrangement is relatively neat, and they contain a large quantity of benzene, phenol, and indole compounds; and (ii) the microscopic particles of water-insoluble IHFM are larger and the arrangement is irregular. The types and quantities of benzene, phenol, and indole compounds are relatively small, rich in a variety of sugar monomers, and may be insoluble in water due to the presence of a greater number of aliphatic groups. Studies have found that water-soluble IHFM has good cellular antioxidant activity, can reduce oxidative damage by hydrogen peroxide (H_2O_2) on LO2 cells effectively and can significantly reduce the level of intracellular reactive oxygen species (ROS) to protect the liver. These results are beneficial in order to develop applications of melanin in the food industry and in other fields.

1. Introduction

Melanin is an aggregation of phenolic and indole substances with extremely complex and heterogeneous chemical structures. It is the most widely distributed and abundant pigment among the known biopigments, and exists widely in various animals, plants, and microorganisms. Depending on the synthetic pathway and intermediate metabolites, the different types of melanin can be divided into eumelanin (with nitrogen and without sulfur atoms; black or brown), brown melanin (with nitrogen and sulfur atoms; brown-black, yellowish brown, or brown), and phaeomelanin (black or brown) (Zhou, 2011). Melanin has excellent thermal stability, photostability, antioxidant, and other physical and chemical properties, with antibacterial, antiviral, radiation resistance, liver damage improvement, DNA protection, and other physiological activities (Chen et al., 2021). El-Naggar and El-Ewasy found that melanin from *Streptomyces glaucescens* NEAE-H can significantly inhibit the activity of skin cancer cells, but has few toxic and side effects on human lung fibroblasts and human amniotic cells (El-Naggar & El-Ewasy, 2017). Shi et al. found that the intracellular melanin of *Lachnum* YM226 not only promoted the apoptosis of liver cancer cells but also had a good hypolipidemia effect, significantly reduced low density lipoprotein cholesterol (LDL-C), and increased the amount of high density lipoprotein cholesterol (HDL-C) in mice, suggesting that natural melanin is a potential anticancer and hypolipidemic active substance (Shi, Li, Ye, et al., 2018; Shi, Li, Yang, Hou, & Ye, 2018). Studies have shown that melanin also has a wide range of industrial

* Corresponding author at: College of Life Sciences, Fujian Agriculture and Forestry University, Fuzhou, Fujian 350002, China.
E-mail address: fujunsheng81@163.com (J. Fu).

https://doi.org/10.1016/j.fochx.2022.100498
Received 18 January 2022; Received in revised form 31 October 2022; Accepted 2 November 2022
Available online 11 November 2022

applications, as well as in medicine, food, cosmetics, and other fields.

Inonotus hispidus (Bull.) P. Karst (1879) is a fungus belonging to the phylum Basidiomycota, the class Basidiomycetes, the subclass Agaricomycetes, the order Hymenochaetales, and the family Hymenochaetaceae, which is rich in polysaccharides, polyphenols, terpenoids, flavonoids, and other active substances (Liu et al., 2019; Yang et al., 2019; Zan and Bao, 2011; Zan et al., 2015). It has good antioxidant, antitumor, hypoglycemic, and other functions. In recent years, melanin derived from fungi such as *Auricularia auricula*, *Boletus griseus Forst*, *Trichoderma* YM404, etc. have attracted widespread interest because of its rapid production, short lifecycle, and high yields, which is conducive to industrial production. The research of *I. hispidus* mainly focus on cultivation of fruiting bodies, chemical components (polysaccharides, flavonoids, triterpenes, etc.) and their pharmacological activities (Li & Bao, 2022). Previous studies have found that *I. hispidus* contains melanin, which has good antioxidant activity to 2,2-diphenyl-1-picrylhydrazyl (DPPH) and hydroxyl radicals. At present, there are few reports on the melanin obtained from *I. hispidus* and few studies of its structure and physicochemical properties. Hou et al. (2019) found that the fruiting body of *I. hispidus* contains melanin, and its solubility, stability (to light, heat, metal ions, etc.), redox, and other physical and chemical properties have been studied. Their results show that melanin has a certain degree of thermal stability and tolerance to light, good solubility under alkaline conditions, and good oxidation resistance to DPPH and hydroxyl radicals. However, the structure of melanin has not been analyzed or determined, and there are few studies on its biological activity.

This study found that the melanin from *I. hispidus* is composed of both water-soluble and water-insoluble forms, its structure wase characterized, and its liver-protective and anticancer activities were further studied. Its chemical composition and structure were characterized by ultraviolet (UV) absorption spectroscopy, Fourier transform infrared (FTIR) spectroscopy, elemental analysis, nuclear magnetic resonance (NMR) spectroscopy, pyrolysis gas chromatography-mass spectrometry (Py-GCMS) and matrix-assisted laser desorption/ionization-time of flight mass spectrometry MALDI-TOF-MS/MS, and their physiological activities were studied. The structure of melanin affects the various aspects of its activity; thus, structural analysis is beneficial for exploring the active site of the molecule. There are many uncertainties about the chemical composition of melanin from different sources, including its chemical insolubility and complex structural diversity. In this regard, the structure of *I. hispidus* melanin has been found to be complex, and its molecular structure is still unclear, which needs further exploration.

2. Materials and methods

2.1. Reagents and instruments

Experimental strain: MS-5(Obtained by our laboratory from the fruit bodies of *I. hispidus* growing on wild jujube trees in Zhongwei City, Ningxia (NCBI login number of ITS sequence: MF183947).

Reagents: DPPH, 2,2′-azino-bis (3-ethylbenzothiazoline-6-sulfonic acid) (ABTS), and Vitamin C (V_C) were purchased from Sigma Company (San Francisco, CA, USA). Anhydrous ethanol, potassium persulfate aqueous solution, salicylic acid, ferrous sulfate, and hydrogen peroxide were all analytically pure grade and were purchased from chemical suppliers in China.

Instruments: Helios G4 CX scanning electron microscope (SEM) (Suzhou Curtis White Industrial Equipment Co., ltd.); Elemantar Vario El Cube (Shanghai) Co., ltd.; UV-5200 ultraviolet spectrophotometer (Shanghai Yuanqing Instrument Co., ltd.); Thermo Scientific Nicolet 10 infrared spectrometer (Wuhan Detmould Technology Co., ltd.); FrontierEGA/PY3030D pyrolysis apparatus (Shanghai Shanpu Electronic Technology Co., ltd.); TRACE1310 gas chromatograph (Jin Heng Instrument (Shanghai) Co., ltd.; ISQ Series single quadrupole chromatograph mass spectrometer (Baidaoheng Instrument Equipment (Beijing) Co., ltd.); Bruker 400 M superconducting nuclear magnetic resonance spectrometer (Zhengzhou Shuren Technology Development Co., ltd.); Varioskan Flash multifunctional enzyme marker (Thermo Scientific, Waltham, MA, USA).

Software: SPSS 25.0 (IBM, Armonk, NY, USA).

2.2. Preparation of melanin

Refer to the method of Hou et al. and other methods with slight modifications (Hou et al., 2019; Yu, Hu, & Ma, 2015). The collected fruiting bodies of *I. hispidus* were dried in an oven at 60 ℃ to constant weight and then pulverized and passed through an 80-mesh sieve. An accurately weighed1.0 g quantity of the fruiting body powder was dissolved in 1.5 mol/L sodium hydroxide (NaOH) at a material-to-liquid ratio of 1:30. After fully reacting for 1 h, the mixture was centrifuged at 10000 rpm for 5 min to collect the supernatant. The pH of the obtained supernatant was adjusted to 1.5–2.0, the latter was placed in a water bath at 80 ℃ for 10 h, and the precipitate was then collected by centrifugation as the crude melanin product. The previous step was repeated, the precipitate was rinsed repeatedly with distilled water until its pH was neutral (7.0), and then rinsed with chloroform, dichloromethane, ethyl acetate, absolute ethanol, 75 % ethanol, and distilled water in sequence and centrifuged at 10,000 rpm for 5 min. From the precipitate obtained, the pure insoluble melanin product was obtained by freeze-drying. The precipitate in the previous step was redissolved with 0.1 mol/L NaOH, which was then adjusted to neutral pH with 0.1 mol/L HCl, dialyzed in running water for 48 h, and freeze-dried to obtain the water-soluble melanin isolate. This method of preparation of water-soluble melanin has been patented (Fu et al., 2019). The calculation of *I. hispidus* fungal melanin (IHFM) yield is given by Equation (1):

$$\textit{Melanin yield}\ (\%) = \textit{Mass of crude melanin}/\textit{Mass of fruiting body powder} \times 100\% \quad (1)$$

2.3. Morphological observation of IHFM

A quantity (10 mg) of melanin powder was sprayed with gold for 50 s to enhance the electrical conductivity of the sample. The sample was then glued in direct contact with a conductive adhesive for testing, and the surface morphology of the melanin powder was observed and photographed with Helios G4 CX Scanning electron microscope.

2.4. Detection of IHFM elements

The C, H, N, and S contents of 50 mg melanin samples were determined using an organic element analyzer. The samples were wrapped in tin foil and burned in the German Elementar Vario EL cube organtic element analyzer. The gaseous products were measured, and the content of each element was calculated.

2.5. Spectral characteristics of IHFM

2.5.1. Detection of IHFM from its UV total absorption spectrum

A quantity of 1 mg of IHFM was weighed out and dissolved in 0.1 mol/L NaOH solution, heated in a water bath at 50–60 ℃ and thoroughly mixed. After 30 min, the pigment had completely dissolved, and the solution was centrifuged at 3000 rpm for 10 min. The supernatant was scanned in the wavelength range 200–700 nm to determine the UV total absorption spectrum (Zhang, Wang, Liu, & Guo, 2016).

2.5.2. Detection of IHFM by FTIR spectroscopy

Referring to the methods of Li et.al (Li et al., 2010). The potassium bromide (KBr) tablet pressing method was adopted. Approximately 1–2 mg of purified IHFM powder and 200 mg of pure KBr powder were

added to the mold and pressed into transparent slices using an oil press, the sample was placed in an infrared spectrometer, Thermo Scientific Nicolet 10. The infrared absorption spectra were determined in the wave number range 4000–400 cm^{-1} at a scanning number of 32 and a resolution of 4 cm^{-1}.

2.5.3. Detection of IHFM by NMR

Water-soluble IHFM was dissolved in deuterium oxide (D_2O) and water-insoluble IHFM was dissolved in deuterated dimethyl sulfoxide (DMSO). The ^1H NMR spectra of both samples were determined using a Bruker 400 M superconducting NMR spectrometer.

2.6. Determination of IHFM by Py-GCMS

The samples were lysed by FrontierEGA/PY3030D thermal cracking apparatus, and the products were analyzed by TRACE1310 gas chromatography and ISQ mass spectrometer.

The conditions of the mass spectrometry scan were: ion source temperature of 300 ℃, transmission line temperature of 320 ℃, and scanning ion range 35–500. The chromatographic conditions were as follows: DB-5 (5% biphenyl–95% polymethylsiloxane) weakly polar quartz capillary column (30 m × 0.25 mm × 0.25 μm); injector temperature: 320 ℃; shunting ratio: 100; carrier gas mode: constant current; carrier gas flow rate: 1.0 mL/min. The GC parameters were kept at 50 ℃ for 2 min, 10 ℃/min to 280 ℃; the temperature was kept at 280 ℃ for 10 min, 20 ℃ to 320 ℃; water-soluble IHFM and water-insoluble IHFM were determined by Py-GCMS at 320 ℃ for 2 min. The NIST database was used.

2.7. Detection of IHFM using MALDI-TOF-MS/MS

Water-soluble IHFM (10 mg) and water-insoluble IHFM (10 mg) were dissolved in 2 mL of 2,5-dihydroxybenzoic acid (DHB) matrix to prepare the 5 mg/mL solution. MALDI-TOF-MS/MS detection of positive ions in samples was performed in linear mode on a bruker ultraflextreme MALDI-TOF-MS/MS instrument.

2.8. Determination of the antioxidant activity of IHFM on cells

2.8.1. Cytotoxicity test of IHFM

Following the method of Liu et al. (Liu et al., 2020), the inoculation density was 1×10^5 cells/mL, and they were inoculated into 96-well plates at a volume of 200 μL per well, with an equal volume of phosphate-buffered saline (PBS) buffer filling at the edges, and cultured under 5 % CO_2 at 37 ℃. After 24 h, the supernatant was removed, and samples of cell culture medium containing 0.05, 0.125, 0.25, 0.5, 1, 2, and 5 mg/mL of water-soluble IHFM was successively added to the experimental group. The blank group only had cell culture medium added; the cell culture medium was added to the control group for normal cell culture. After 24 h, the supernatant was removed and 90 μL of cell culture medium and 10 μL of 10 % 3-[4,5-dimethylthiazol-2-yl]-2,5-diphenyltetrazolium bromide (MTT) solution were added to each sample. After 4 h, the supernatant was removed, 150 μL of DMSO was added, and the mixture was mixed using vigorous shaking for 15 min to avoid light contamination. The absorbance values of each group were measured at 490 nm. The cell survival rate was calculated from the optical density (OD) using Equation (2):

$$\text{Cell survival rate}\,(\%) = \frac{\text{OD experimental group} - \text{OD blank group}}{\text{OD control group} - \text{OD blank group}} \times 100\% \quad (2)$$

2.8.2. Oxidative damage caused by H_2O_2 on LO2 cells

Following the method of Liu et al. (Liu et al., 2020), cell planking was performed in the same way as in their section 2.8.1. The blank group only had PBS buffer added; the cells in the control group were cultured for 2 h after being added to the medium. Following the end of cell culture, the supernatant was removed and 90 μL of cell culture medium and 10 μL of 10 % MTT solution were added to each group. After 4 h of culture, the supernatant was removed and 150 μL of DMSO was added. After 15 min of vigorous shaking, the absorbance of each group was measured at 490 nm. Finally, the median inhibitory concentration (IC_{50}) of the cells was calculated using SPSS 25.0 software.

2.8.3. Effect of IHFM on oxidative damage to LO2 cells

Referring to the method of Qi et al. (Qi et al., 2018), the cell slab used was the same as described in their section 2.8.1. Following the end of cell culture, the supernatant was removed, and the experimental groups were added to cell media containing different concentrations of water-soluble IHFM (0.05, 0.125, 0.25, 0.5, 1, 2, and 5 mg/mL). The blank group, control group, and model group were added to complete the medium and cultured for 24 h. Following cell culture, the supernatant was removed. To each experimental group and model group, 200 μL of H_2O_2 was added to cause the LO2 cells to reach the 50 % inhibition concentration, 200 μL of PBS buffer was added to the control group, and 200 μL of PBS buffer without cells was added to blank group. In each experimental group and model group, 200 μL of H_2O_2 was added at a concentration of 50 % inhibition of LO2 cells, 200 μL of PBS buffer was added to the control group, and 200 μL of PBS buffer without cells was added to the blank group. The cell morphology was observed after 2 h of culture time, the supernatant was discarded, and 90 μL of cell medium and 10 μL of 10 % MTT solution were added to each group. After 4 h of culture, the supernatant was removed, 150 μL of DMSO was added, and the absorbance of each group was measured at 490 nm after 15 min of vigorous shaking. The cell survival rate was calculated using Equation (2) above.

2.9. Statistical analysis of the data

The experimental data were analyzed using SPSS 25.0 statistical software. The measured data ($x \pm$ SD) are the mean ± standard deviation. The significance of the data was analyzed by one-way of variance (ANOVA), $p < 0.05$ represents a significant difference, while $p < 0.01$ represents an extremely significant difference.

3. Results

3.1. Differences in microstructure under scanning electron microscopy (SEM)

In the precious studies, we have optimized the melanin extraction process and solid fermentation conditions of the fruiting body of *I. hispidus*, and found that the best way to extract IFHM is the complex enzymatic method, and the yield of IFHM can reach 23.73 ± 0.57 %, which is equivalent to 1.27 times before optimization (Zhang et al., 2021). After obtaining the best solid medium formulation by optimizing the solid fermentation conditions, the yield of IFHM can reach 31.80 ± 1.34 %, which is equivalent to 1.7 times that before optimization (Zhang et al., 2021).

We first observed the fine structure of melanin particles using transmission electron microscopy (TEM). Morphological observation showed that the water-soluble IHFM obtained following separation and purification of *I. hispidus* melanin was a black powder with a uniform texture and luster (Fig. 1A). The water-insoluble IHFM was a brown powder with a uniform texture but no luster (Fig. 1B). By observing and analyzing the ultrastructure of *I. hispidus* melanin, the morphologic differences between water-soluble and water-insoluble IHFM were further explored. As shown in Fig. 1, the microstructures of soluble and water-insoluble IHFM were significantly different. Water-soluble IHFM has a smooth surface and is composed of spherical particles with diameters of 10–15 nm arranged in irregular planes (Fig. 1). Water-soluble

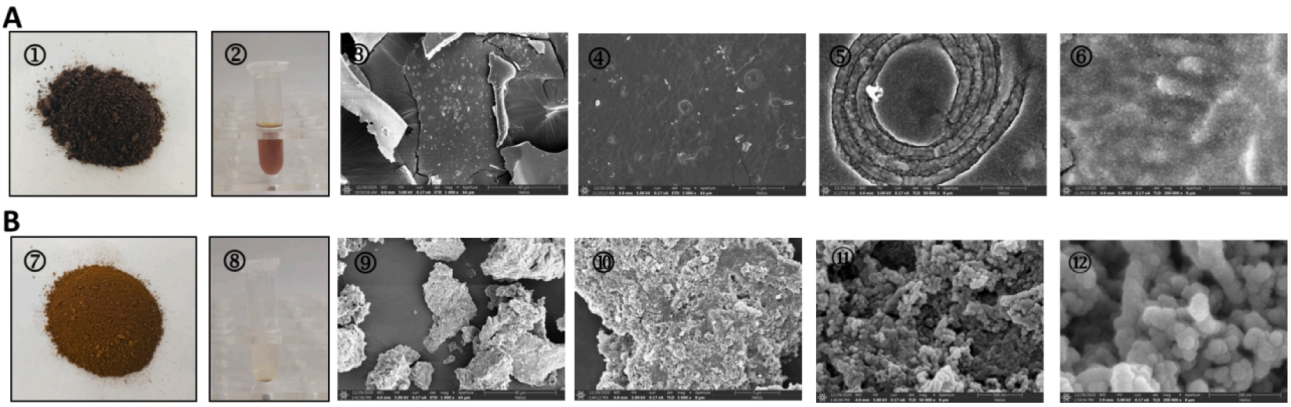

Fig. 1. Morphological characteristics and scanning electron micrographs of the melanin obtained from *I. hispidus*. (A): Water-soluble IHFM: ①water-soluble melanin powder; ②5 mg of powder dissolved in 1 mL of water; ③–⑥ microstructure of melanin, which is surrounded by concentric layers of circular units. (B): Water-insoluble IHFM: ⑦water-insoluble melanin powder; ⑧The latter is insoluble in water, and there is a powder residue at the bottom of the centrifuge tube; ⑨–⑫microstructure of melanin, with an irregular arrangement.

melanin contains circular units in a heterogeneous mass wrapped in thick-walled concentric layers. As shown in Fig. 1B, water-insoluble IHFM is mainly lumpy, with a rough surface, and stacked with 35–50 nm spherical particles into an irregular three-dimensional structure, indicating that the morphological characteristics of both water-soluble and water-insoluble IHFM are quite different. To sum up, it can be seen that the microstructure of *I. hispidus* melanin may not have a regular distribution pattern.

3.2. Differences in atom type and content of water-soluble and water-insoluble melanin

We then determined the elemental composition of melanin by means of elemental analysis, which succeeded in determining the main elements of IHFM, C, H, N, S, and O, and which is an important method for preliminary identification of melanin types. Of these, eumelanin contains N but no S, brown melanin contains both N and S, and phaeomelanin does not contain nitrogen (Nicolaus, 1968). As listed in Table 1, water-soluble and water-insoluble IHFM both contain C, H, N, and O, but do not contain S, indicating that *I. hispidus* melanin is the eumelanin type. The H and O contents of both soluble and water-insoluble IHFM are similar, while the C and N contents differ greatly. The C/N ratio of water-insoluble melanin was higher than that of water-soluble melanin, indicating that there were more aliphatic groups and carboxyl monomers in the structure of insoluble melanin.

3.3. Spectral characteristics of IHFM

3.3.1. UV total absorption spectral analysis of IHFM

The UV total absorption spectra of water-soluble and water-insoluble IHFM were measured using a UV spectrophotometer, and it was found that the maximum absorption peak occurred at 226 nm in the UV region, and the absorbance gradually decreased toward the visible region (Fig. 2A), which was consistent with the absorption characteristics of melanin. Accordingly, as shown in Fig. 2B, a standard curve was drawn up for the melanin in the fruiting body of *I. hispidus*, with the IHFM concentration as the horizontal coordinate and absorbance as the vertical coordinate. The regression equation for water-soluble IHFM was obtained as: $y = 6.634x + 0.0695$, and the correlation coefficient was $R^2 = 0.9935$. The regression equation for water-insoluble IHFM was: $y = 6.492x + 0.072$; $R^2 = 0.9954$, indicating that the purity of the extracted IHFM was high.

Table 1
Elemental composition of *Inonotus hispidus* melanin.

Element	Soluble melanin	Insoluble melanin	Eumelanin*	Phaeomelanin*
C	41.36	43.67	56.45	46.24
H	6.203	6.251	3.15	4.46
N	5.87	3.5	8.49	9.36
S	0	0	0.09	9.78
O	46.567	46.579	31.82	30.16

* Represents cited reference (Ito & Fujita, 1985).

3.3.2. Infrared spectral analysis of IHFM

Infrared spectral analysis is one of the commonly used methods for analyzing the chemical structures of molecules, and each functional group has a specific infrared absorption peak (Zhang, Zhang, Zhang, Ai, & Huang, 2011). As shown in Fig. 2C, the infrared spectra of soluble and water-insoluble IHFM had the same main absorption peaks. The characteristic absorption peaks at 3396.17 and 3425.1 cm^{-1} were strong and broad, corresponding to the –NH group connected to the –OH group of the indole ring. The peaks at 2921.75 and 2927.54 cm^{-1} correspond to aliphatic C—H. The peak at 1637.34 cm^{-1} corresponds to C═O stretching or aromatic C═C stretching. The peak around 1521.62 cm^{-1} is related to the N—H bending vibration. The peak values of 1407.84 and 1376.98 cm^{-1} are related to the tensile peaks of –CN, suggesting that the indole structure is present. The weak absorption band at 673.06 cm^{-1} indicates that the aromatic ring has become a conjugated system. The above characteristics indicate that the infrared spectrum of IHFM obtained by extraction and purification conforms to the structural characteristics of traditional melanin.

3.3.3. Nuclear magnetic resonance (NMR) analysis of IHFM

The NMR hydrogen spectrum is one of the most sensitive NMR spectra and is commonly used to characterize the number and type of hydrogen atoms in compounds. As shown in Fig. 3A and 3B, water-soluble IHFM has four obvious peak groups, the rest are continuous peak groups, and water-insoluble IHFM has eight main peak groups. The peaks at 2.5 and 4.75 ppm are solvent absorption peaks; the peak in the range 0–2.5 ppm usually belongs to the C—H tensile vibration signal peak of an alkyl segment. Peaks between 3.2 and 4.2 ppm correspond to $–CH_2$ or $–CH_3$ groups on nitrogen or oxygen atoms; the peak between 4.2 and 5.4 ppm is caused by the —C═C—H group connected to nitrogen or oxygen atoms; the peak in the range 6.8–8.5 ppm is the aromatic hydrogen in the indole or pyrrole ring, indicating that the hydrogen spectra of soluble and water-insoluble IHFM are significantly different.

3.4. Analysis of IHFM by Py-GCMS

Py-GCMS can be used to obtain the structural monomers of complex compounds from their pyrolysis products. Previous studies have shown

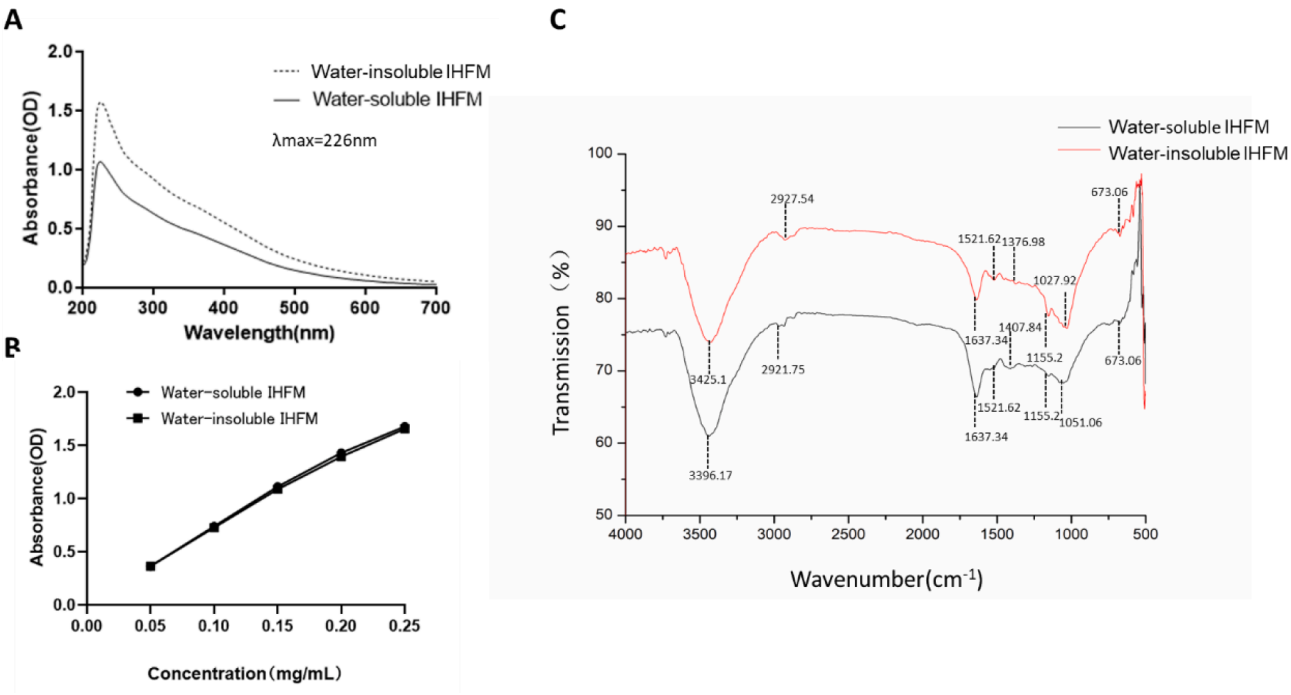

Fig. 2. UV and FTIR spectra of the melanin from *I. hispidus*. (A) The maximum UV total absorbance of *I. hispidus* melanin was detected at 226 nm. (B) Standard curve for *I. hispidus* melanin. (C) Fourier Transform infrared spectroscopy of *I. hispidus* melanin.

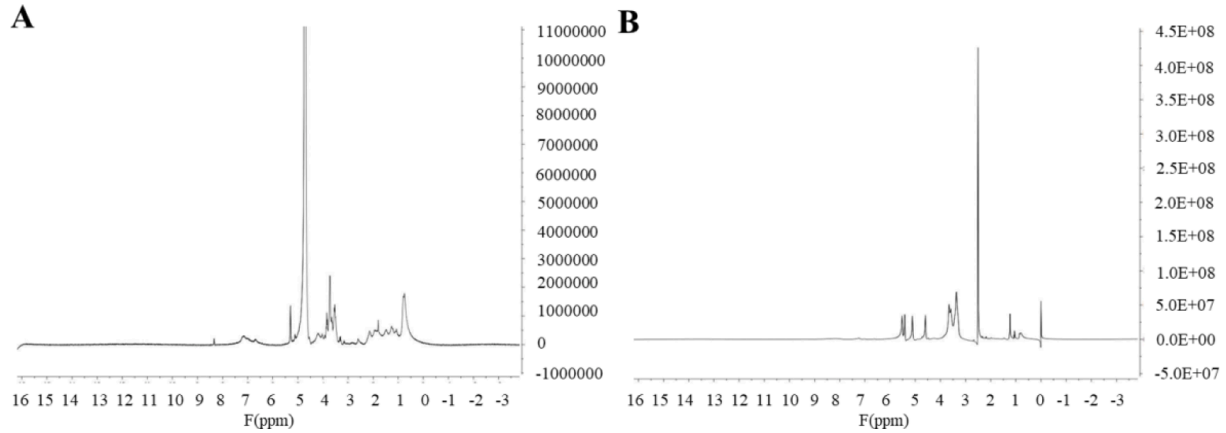

Fig. 3. ^{1}H NMR spectrum of IHFM. (A) Water-soluble melanin; (B) Water-insoluble melanin.

that benzene, phenol, indole, pyrrole, and their derivatives are the most significant characteristic thermal degradation products of eumelanin (Liu, Xiao, Liu, Zhuang, & Sun, 2018). On the basis of clarifying the constituent elements, characteristic functional groups, and types of hydrogen atoms in the IHFM in our study, Py-GCMS was further used to determine the structural components of the water-soluble and water-insoluble IHEM (Fig. 4A and 4B). As listed in Table 2, by noting compounds with a peak area of 1 % or more, it was found that water-soluble IHFM contains a large number of benzene, phenol, and indole groups, consistent with the characteristics of eumelanin (Ai, Tanabe, & Nishimura, 2003). As listed in Table 3, the types of benzene, phenol, and indole compounds found in water-insoluble IHFM were fewer than those of water-soluble IHFM, but were rich in a variety of carbohydrate monomers, indicating that water-soluble IHFM has more characteristic components of melanin than water-insoluble IHFM.

3.5. Mass spectrometry analysis of IHFM

MALDI-TOF-MS/MS was used to determine the water-soluble and water-insoluble IHFMs of *I. hispidus* in order to analyze the structural characteristics of melanin. As shown in Fig. 4C and 4D, the main ion peaks of water-soluble and water-insoluble IHFM were basically the same, with the relative molecular mass of the two likely to be 271, but different fragment ion peaks were also present. The water-soluble melanin and water-insoluble melanin can be distinguished. The maximum mass-charge ratio of water-soluble melanin is $[M + H]^{+}$ m/z = 272.2434, and the major fragment ion peaks are 43.1307, 57.1598, 58.1575, 137.1438 and 271.9993 respectively. The maximum mass-charge ratio of water-insoluble melanin is $[M + H]^{+}$ m/z = 272.0308, and the following fragment ion peaks can be obtained: 30.1051, 43.1319, 46.1447, 57.1502, 58.1497, 137.1375. In conclusion, the relative molecular mass of water-soluble melanin and water-insoluble melanin may be 271, but different fragment ion peaks can be obtained by MALDI-TOF-MS/MS, and their mass-to-charge ratios are also

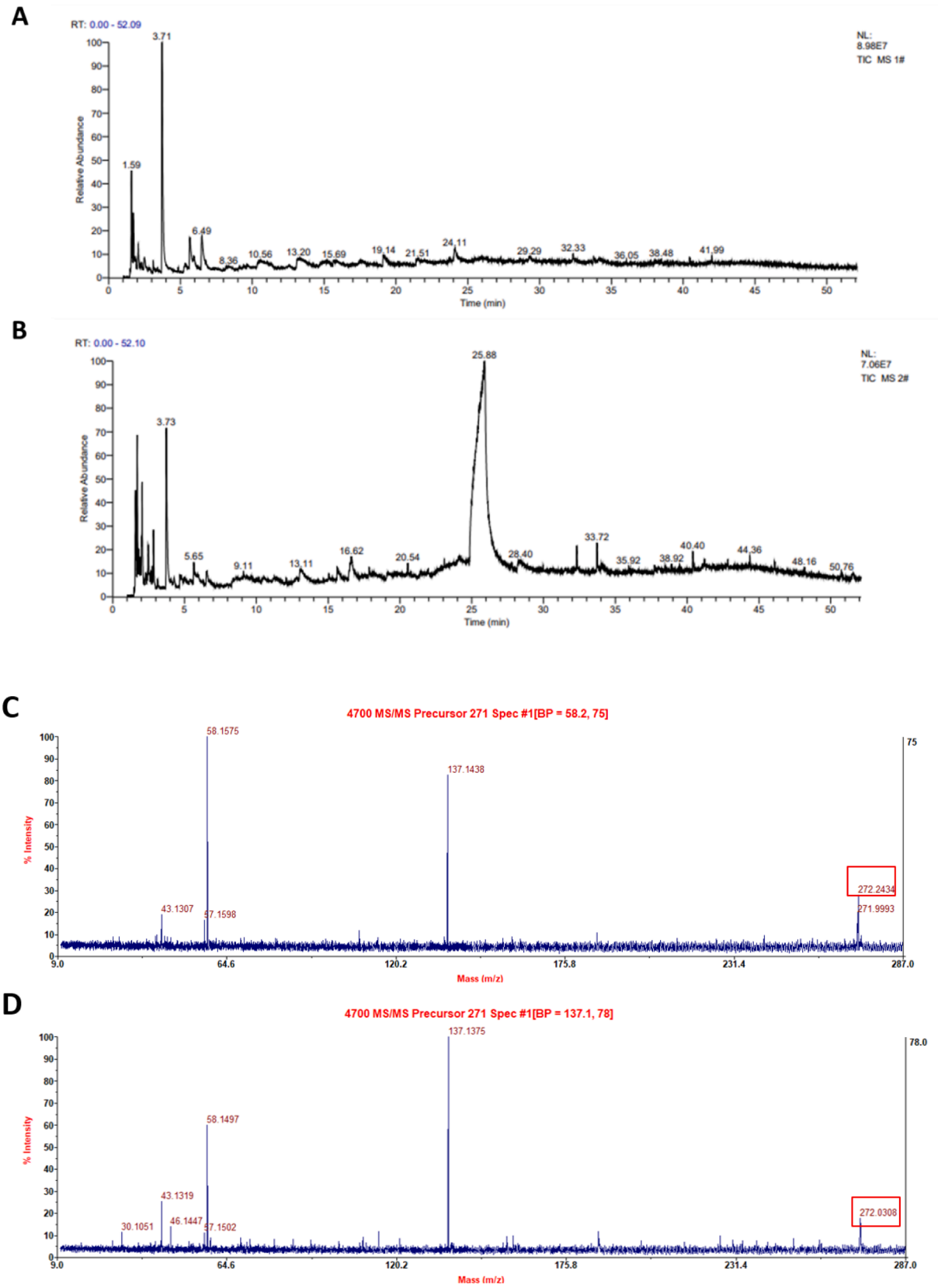

Fig. 4. Pyrolysis product analysis of water-soluble and water-insoluble IHFM. (A) Product analysis peak of thermal cracking of water-soluble IHFM; (B) Product analysis peak of thermal cracking of water-insoluble IHFM. Water-insoluble IHFM has more peaks than water-soluble IHFM. (C) Mass spectrum of water-soluble IHFM. (D) Mass spectrum of water-insoluble IHFM.

Table 2
Composition of water-soluble melanin compounds from *Inonotus hispidus*.

RT (min)	Compound name	S/N	Area (%)
3.71	Methylbenzene	18398.86	21.42
1.59	DL-2-aminoadipic acid, methanethiol	7501.55	7.60
1.71	1-Methylcyclopropanemethanol, *N*-methyl-L-leucine, sulfocyanic acid	4834.62	7.53
6.49	Styrene, bicyclo[4.2.0]octa-1,3,5-tetraen	2415.71	4.02
5.65	Ethylbenzene	2288.71	3.43
2.06	3-Cyclopentene-1,2-diol, 5-methyl-1H-pyrazole, 2-cyclopentenone, 3-methylfuran	1892.73	2.41
3.10	(S)-(+)-2-Methylbutyronitrile, 3-oxo-1,8-octane dicarboxylic acid, L-valine, L-(+)-threose, amastatin	951.33	0.92
2.49	Benzene, 2-bromo-4,5-methylenedioxymethamphetamine	942.55	1.47
24.11	*N*-Benzyl-1-cyclopropyl-2-methyl-5-oxpyrrolidine-2-carboxyamide, M-nitrocarbamate, 1,1′-bi(cyclohexyl), 2-(2-methylpropyl), 2-methyl-*n*-(1-octahydroquinolinzine-1-ylmethyl)-benzamide, 2-butyl-1,1′- dicyclohexyl	807.96	1.92
13.19	4-Methylphenol	771.72	5.85
19.14	Indole	685.86	1.88

Table 3
Composition of water-insoluble melanin compounds from *Inonotus hispidus*.

RT (min)	Compound name	S/N	Area (%)
3.73	Methylbenzene	7805.21	9.28
1.7	3-Aminopyrrolidine-3-carboxylicacid, clomipramine- *N*-oxide, imipramine-*N*-oxide, 1-penten-3-ol	6387.69	5.19
2.05	3-Methylfuran, 5-methyl-1H-pyrazole	4446.31	4.87
1.59	Oxprenolol, pindolol, *N, N*-hexamethylene thiocarbamate-s-ethyl ester, 4-hydroxy propranolol, esmolol hydrochloride	4403.46	4.53
25.91	1,6-Anhydro-beta-D-glucose, D-glucopyranose, D-allose	3910.51	10.13
2.84	2,5-Dimethylfuran	2643.57	2.48
2.48	2-Bromo-4,5-methylenedioxymethamphetamine, benzenesulfonic acid, 2-[(5-bromo-2-hydroxy-phenyl) methylene] hydrazide, benzeneethanol, 3-nitrophenethyl alcohol	1866.92	2.55
33.73	(E)-2-Methylbut-2-en-1-ylmethacrylate, 2,6-octa-dien-1-ol, 3-methyl-3-buten-1-ol	1374.14	1.44
24.98	1,6-Anhydro-beta-D-glucose, D-glucopyranose, D-allose	1275.43	2.75
32.31	2-Pentadecylfuran, 2-tridecylfuran	1275.17	1.55
25.04	1,6-Anhydro-beta-D-glucose, D-glucopyranose, D-allose	1228.97	2.25

different, that the structural formula are different.

3.6. Hepatoprotective activity of water-soluble IHFM

The antioxidant activity of water-soluble IHFM was further explored by constructing the oxidative damage model for LO2 liver cells. Water-soluble IHFM was taken as the experimental object and the MTT test was performed on LO2 cells. It was found that water-soluble IHFM had no significant effect on the proliferation of LO2 liver cells (Fig. 5C), indicating that water-soluble IHFM had no obvious toxic and side effects on liver cells. H_2O_2 is a common reactive oxygen species, which readily reacts with the iron ions in living cells to form free radicals and cause damage, including cell lipid peroxidation. Therefore, H_2O_2 is often used as an inducer for building oxidative damage models (Dai et al., 2017). As shown in Fig. 5A, with increasing hydrogen peroxide concentration, the number of LO2 cells gradually decreased, the adhesion of LO2 cells also decreased, and the cell morphology became rounded. Moreover, as shown in Fig. 5D, the survival rate of LO2 cells decreased in a dose-dependent manner with increasing hydrogen peroxide concentration, the IC_{50} value was 1.577 mmol/L, indicating that H_2O_2 seriously affected the growth of LO2 cells.

Under conditions of 1.577 mmol/L H_2O_2 concentration, the protective effect of water-soluble IHFM on oxidative damage to LO2 cells was further explored. As shown in Fig. 5B, D, and E, LO2 cells in normal culture had a good morphology, a large number of living cells, good adhesion, and uniform distribution (Fig. 5B), and low relative ROS content (Fig. 5F). Compared with the blank group, the cell morphology of the model group was shriveled, a large number of cells floated and became rounded (Fig. 5B), and the cell survival rate decreased significantly (Fig. 5E), while the relative ROS content of cells increased significantly (Fig. 5F). Compared with the model group, the morphology of LO2 cells in the experimental group treated with water-soluble IHFM was significantly improved (Fig. 5B). When the water-soluble IHFM concentration was greater than 0.25 mg/mL, the cell survival rate was significantly increased (Fig. 5E). When the concentration of IHFM was greater than 0.05 mg/mL, the relative ROS content of LO2 cells was significantly reduced (Fig. 5F), indicating that water-soluble IHFM improved the degree of protection against oxidative damage to LO2 cells effectively.

3.7. Anticancer activity of water-soluble IHFM

The MTT experiment was used to detect the cell viability of water-soluble IHFM on MCF-7, HepG-2, and MDA-MB-231 cells (Fig. 6). It has been shown that water-soluble IHFM has certain anti-cancer activities against different cancer cells, and that it has certain inhibitory effects on the proliferation of human liver cancer cells (HepG-2), human breast cancer cells (MCF-7), and human breast cancer cells (MDA-MB-231). The median inhibitory concentrations (IC_{50}) of water-soluble IHFM against these three types of cancer cells were 4.99, 1.413, and 9.833 mg/mL, respectively.

4. Discussion

Melanin has several beneficial medicinal effects. Analysis of its chemical structure is helpful for elucidating the mechanism of its medicinal action. However, the specific structure of fungal melanin has not yet been elucidated, so it is very important to continue to explore its structural characteristics. UV absorption spectroscopy is an important method for identifying the physicochemical characteristics of melanin. Studies have shown that melanin has a maximum absorbance in the UV region, which gradually decreases toward the visible region (Chen et al., 2021). By observing the characteristic infrared absorption peak of melanin, various chemical bonds and functional groups contained within the molecule can be determined by FTIR spectroscopy (Zhang, Zhang, Zhang, Ai, & Huang, 2011). In addition, mass spectrometry is commonly employed for structural analysis of chemical compounds. Benzene, phenol, indole, pyrrole, and their derivatives are the most significant thermal degradation products of eumelanin. Quinoline and isoquinoline molecules are unique thermal degradation products of brown melanin (Liu, Xiao, Liu, Zhuang, & Sun, 2018).

In previous studies, Song performed elemental analysis, ^{1}H NMR and mass spectrometry on *Lachnum* YM226 melanin and found that eumelanin was the main component (Song, Li, Su, Li, Shi, & Ye, 2016). Liu et al. conducted UV–vis absorption spectroscopy, FTIR spectroscopy, elemental analysis, NMR, Py-GCMS, and ultra-high performance liquid chromatography high-resolution mass spectrometry (UHPLC-HRMS) on *Boletus* melanin and found that its structure was composed of 5,6-dihydroxyindole and its derivatives; its polycondensation molecular formula is $[C_{28}(OR_1)_4(OR_2)_3H_{11}O_6N_4]_n$ (Liu et al., 2018). Sun found that the melanin from *Auricularia auricula* is eumelanin and speculated that its polycondensation molecular formula is $([C_{18}(OR)_3H_7O_4N_2]_n)$ (Sun, Zhang, Chen, Zhang, & Zhu, 2016).

In this study, the structural characteristics of soluble and water-

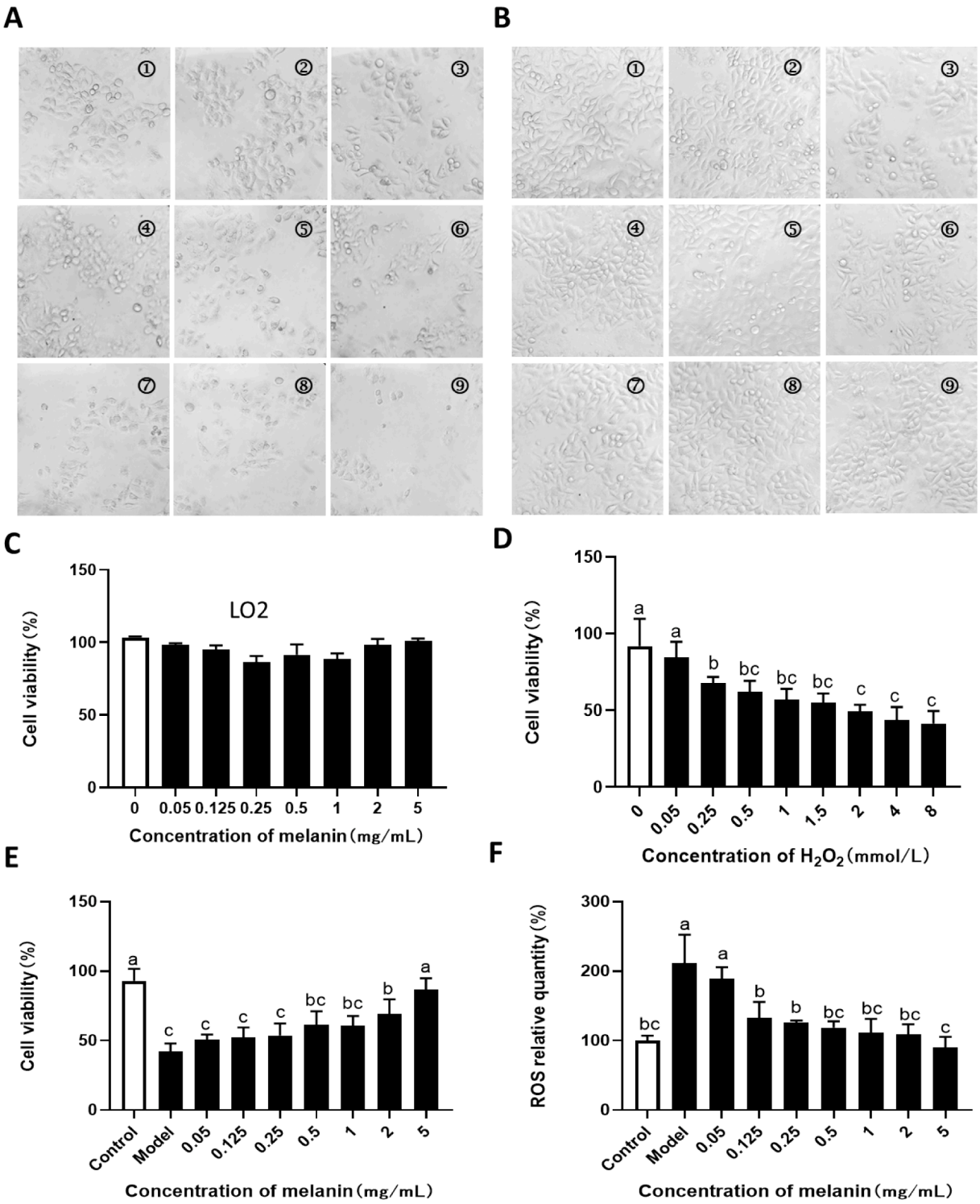

Fig. 5. Protective effect of water-soluble IHFM on LO2 cells damaged by H_2O_2. (A) (①–⑨) cell morphology of cells treated with H_2O_2 concentrations of 0, 0.05, 0.25, 0.5, 1, 1.5, 2, 4, and 8 mmol/L. (B) ①–⑨) Using a H_2O_2 concentration of 1.577 mmol/L, water-soluble IHFM treated 0.05, 0.25, 0.5, 1, 1.5, 2, 4 and 8 mg/mL LO2 cell morphology. (C) Effects of different water-soluble IHFM on the viability of LO2 cells. (D) Effect of H_2O_2 on LO2 cells. (E) Effect of water-soluble IHFM on the cell viability of oxidatively injured LO2 cells. (F) Effect of water-soluble IHFM on the relative quantity of ROS in oxidatively injured LO2 cells. Note: Different lowercase letters indicated significant difference between groups ($p < 0.05$).

insoluble IHFM were detected using SEM, UV total absorption spectroscopy, FTIR spectroscopy, elemental analysis, NMR, Py-GCMS, and MALDI-TOF-MS. It was found that both water-soluble and water-insoluble IHFM have maximum absorption values at 226 nm, which belong to eumelanin, and their maximum mass–charge ratios are $[M + H]^+$ m/z = 272.2434 and 272.0308, respectively. The relative molecular mass of water-soluble IHFM and water-insoluble IHFM could be 271. However, there are differences between water-soluble IHFM and water-insoluble IHFM in microstructure, element composition and structure composition. Water-soluble IHFM is spherical particles with a diameter of 10–15 nm and a smooth sheet on the surface, while water-insoluble IHFM is spherical particles with a diameter of 35–50 nm and

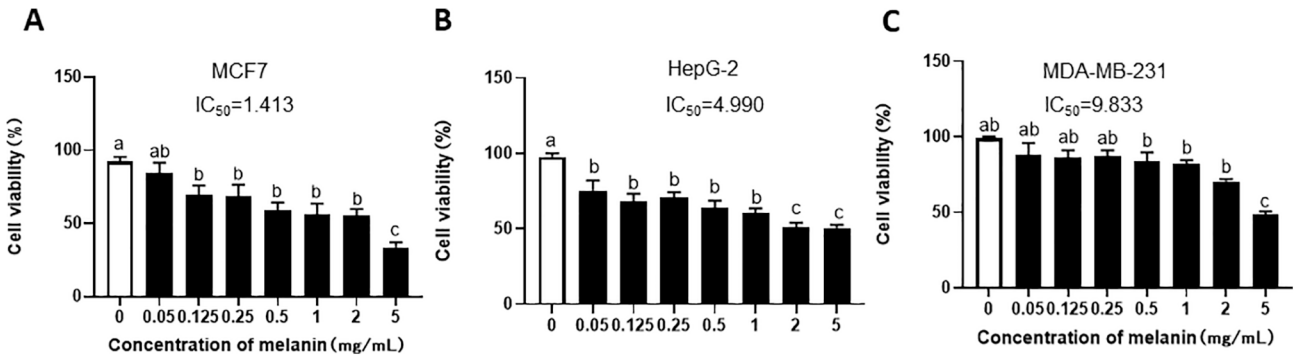

Fig. 6. Evaluation of anti-cancer activity of water-soluble IHFM on MCF-7, HepG-2, and MDA-MB-231 cells. (A) Water-soluble melanin can affect the vitality of MCF-7 cells. When water-soluble IHFM was used to treat MCF, the concentration of 1.413 mg/mL can reached the half-lethal rate. (B) The median lethal concentration of water-soluble IHFM treatment of HepG-2 was IC_{50} = 4.99 mg/mL. (D) The Effect of water-soluble IHFM on the viability of MDA-MB-231 cells. Note: Different lowercase letters indicated significant difference between groups ($p < 0.05$).

a rough block on the surface, this may be due to the presence of water insoluble substances in the IHFM particles. Although both water-soluble IHFM and water-insoluble melanin are eumelanin, the C/N ratio of water-insoluble IHFM is higher than that of water-soluble melanin, the results show that there are more aliphatic groups and carboxyl monomers in the water-insoluble IHFM structure. The results of MALDI-TOF-MS/MS analysis showed that the fragment ion peaks and mass-charge ratios of the two species were different, which may be due to the different R groups in their structures, it is further shown that the structural formula of water-soluble IHFM is different from that of water-insoluble IHFM. The results of Py-GCMS analysis showed that water-soluble IHFM contains a large number of benzene, phenol, and indole characteristic compounds, while water-insoluble IHFM contains fewer benzene, phenol, and indole compounds and a variety of carbohydrate monomers, indicating the higher purity of water-soluble IHFM.

In the preliminary study, the solid-state fermentation method optimized the production of melanin of *Inonotus hispidus*, optimized the melanin extraction process by ultrasonic method and complex enzyme method, and characterized its physical and chemical properties (Hou, Xin, Xiang, Chen, & Fu, 2018; Zhang et al., 2021). Hou et al. (Hou et al., 2019) showed that IHFM has good stability (light, heat, metal ions, etc.), strong oxidation resistance, and only high temperatures and Cu^{2+} ions affect its stability, which is also consistent with the research of Zhang (Zhang & Zhang, 2006), Wang (Wang et al., 2021) and Yang (Yang, 2019) et al. Under external stimulation, compounds are prone to form groups and atoms without pairs of electrons, called free radicals (Li, 2018). Studies have shown that excessive numbers of free radicals in the body can induce aging, cancer, and other diseases, and the development of effective and active antioxidant substances can help reduce oxidative damage (Zhu et al., 2015). Melanin has good chemical antioxidant activity *in vitro*, and its antioxidant activity and anticancer activity were further explored in this study. Studies have found that water-soluble IHFM can clear ROS produced by H_2O_2 and reduce ROS in LO2 cells, thereby protecting hepatocytes. Water-soluble IHFM can reduce the survival rate of cancer cells such as HepG-2, MCF-7 and MDA-MB-231 and has potential anti-cancer effects, which is consistent with Shi et al.'s discovery that *Lachnum* YM226 melanin has anti-H22 liver cancer effects (Shi et al., 2018).

Structure is closely related to activity, and heterocycles are the key molecular components of most natural products and have important biological activities. Among them, indoles are the most important heterocyclic compounds naturally occurring in drug discovery (Wang, Wang, Long, Wang & Ouyang, 2022). They consist of a phenyl ring and a pyrrole ring. They have low toxicity, high biocompatibility and a variety of pharmacological activities, such as antibacterial, anti-inflammatory, anti-tumor, anti-oxidation. But melanin is a kind of phenolic or indole polymer. By Py-GCMS analysis, the pyrolysis products of *I. hispidus* melanin contain phenol, indole and other products, which accord with the characteristics of true melanin. The melanin of *I. hispidus* has strong stability (light, heat, metal ions, etc.), anti-oxidation and anti-tumor activities, which may be due to its indole ring structure. Because the pyrrole ring in the indole ring is electron-rich, it can form hydrogen bonds with other molecules through π-π stacking in the-NH portion. Indole derivatives play an important role in the research and development of anti-tumor drugs, such as Vinorelbine (Cros et al., 1989), Rucaparib (Anderson et al., 2016), melatonin (Prieto-Domínguez et al., 2017) and so on. In conclusion, water-soluble IHFM can be used as a natural pigment, liver-protective and anticancer drugs, antioxidants in food, medicine, chemical industry and other fields.

5. Conclusions

In this study, water-soluble and water-insoluble IHFM was obtained from the fruiting bodies of *I. hispidus*, and its structure and liver protection may be studied. Both water-soluble and water-insoluble IHFM had maximum absorption values at 226 nm, characteristic of eumelanin, and the maximum mass–charge ratios were $[M + H]^+$ m/z = 272.2434 and 272.0308, respectively. Water-soluble and water-insoluble IHFM are quite different in terms of electron microstructure and structural composition. Among them, the water-insoluble IHFM may not be easily soluble in water due to its large particles, rich in various sugar monomers, and aliphatic groups. It was found that water-soluble IHFM has strong *in vitro* chemical antioxidant activity. This study will study its protective effect on H_2O_2 damage to hepatocytes. IHFM has good *in vitro* antioxidant activity, which can reduced oxidative damage by H_2O_2 on liver cells effectively and significantly reduce the ROS level of cells. This research lays the foundation for the structural characterization of water-soluble and insoluble IHFM of *I. hispidus*, and also provides a theoretical basis for the development and utilization of water-soluble IHFM, which can be used in the fields of food antioxidant, liver protection product development, cosmetics and other fields.

CRediT authorship contribution statement

Xiaomin Li: Conceptualization, Methodology, Software, Data curation, Visualization, Writing – original draft, Writing – review & editing. **Wenya Wu:** Conceptualization, Methodology, Software, Data curation. **Fengpei Zhang:** Conceptualization, Methodology, Data curation. **Xin Hu:** Software, Data curation. **Yuan Yuan:** Writing – original draft, Visualization, Investigation. **Xiaoping Wu:** Visualization, Supervision, Investigation. **Junsheng Fu:** Data curation, Visualization, Investigation, Supervision, Writing – review & editing.

Declaration of Competing Interest

The authors declare that they have no known competing financial interests or personal relationships that could have appeared to influence the work reported in this paper.

Data availability

Data will be made available on request.

Acknowledgment

This work was supported by the Fujian Provincial Department of Science and Technology (No. 2019N0006).

References

Ai, S., Tanabe, S., & Nishimura, T. Antioxidant activity of peptides obtained from porcine myofibrillar proteins by protease treatment. *Journal of Agricultural and Food Chemistry*, *51*(12) (2003), 3661–67.

Anderson, R. C., Makvandi, M., Xu, K., Lieberman, B. P., Zeng, C., Pryma, D. A., et al. (2016). Iodinated benzimidazole PARP radiotracer for evaluating PARP1/2 expression *in vitro* and *in vivo*. *Nuclear Medicine and Biology, 43*(12), 52–758.

Chen, Y., Xu, M., Wang, X. Y., Shan, X. H., Ji, L. K., & Zhang, Y. J. (2021). Summary of melanin of *Auricularia auricula*. *Journal of Hainan Normal University (Natural Science), 34*(1), 63–69.

Cros, S., Wright, M., Morimoto, M., Lataste, H., Couzinier, J. P., & Krikorian, A. (1989). Experimental antitumor activity of Navelbine. *Seminars in Oncology, 16*(2 Suppl 4), 15–20.

Dai, Y. H., Zhang, L. M., Yang, S. X., Yang, X. J., Long, X. Q., Yuan, J. Q., et al. (2017). Protective effect of pollen pini on H_2O_2-induced oxidative damage in HepG2 cells. *Chinese Journal of Experimental Traditional Medical Formulae, 23*(19), 167–173.

El-Naggar, E. A., & El-Ewasy, S. M. (2017). Bioproduction, characterization, anticancer and antioxidant activities of extracellular melanin pigment produced by newly isolated microbial cell factories *Streptomyces glaucescens* NEAE-H. *Scientific Reports, 7*, 42129.

Fu, J.S., Liu, X., Hou, R.L., Qi, M., Lin, W.X. & Zheng, Mi.F. A preparation method of water-soluble fungus melanin [P]. Fujian Province: CN108841200B, 2019-11-15.

Hou, R., Liu, X., Xiang, K., Chen, L., Wu, X., Lin, W., et al. (2019). Characterization of the physicochemical properties and extraction optimization of natural melanin from *Inonotus hispidus* mushroom. *Food Chemistry, 277*, 533–542.

Ito, S., & Fujita, K. (1985). Microanalysis of eumelanin and pheomelanin in hair and melanomas by chemical degradation and liquid chromatography. *Analytical Biochemistry, 144*(2), 527–536.

Li, Q., Hou, L. H., Liu, X., Li, W. L., & Ma, A. M. (2010). Identification and extraction technology of melanin from *Auricularia auricula*. *Food Science, 31*(16), 87–92.

Li, Y. (2018). *Radical-initiated unsaturated hydrocarbon functionalization reactions*. Hunan University.

Li, Z., & Bao, H. (2022). Research advances on chemical constituents and pharmacological effects of traditional Chinese medicine Sanghuang– Inonotus hispidus. *Journal of Fungal Research, 20*(03), 203–213.

Liu, Q. M., Xiao, J. J., Liu, B. T., Zhuang, Y. L., & Sun, L. P. (2018). Study on the preparation and chemical structure characterization of melanin from *Boletus griseus*. *International Journal of Molecular Sciences, 19*(12), 3736.

Liu, X., Hou, R. L., Xu, K. Q., Chen, L., Wu, X. P., Lin, W. X., et al. (2019). Extraction, characterization and antioxidant activity analysis of the polysaccharide from the solid-state fermentation substrate of *Inonotus hispidus*. *International Journal of Biological Macromolecules, 123*, 468–476.

Liu, C. Y., Yuan, Y., Hao, X. Y, Liu, K., Wu, X. P., & Fu, J. S. (2020). A comparative study of intracellular and extracellular polysaccharides in mycelia of *Cordyceps cicadae* against oxidative damage of hepatocvtes. *Mycosystema, 39*(02), 421–433.

Nicolaus, R. A. (1968). *Melanins* (pp. 1–310). Paris: Hermann Press.

Prieto-Domínguez, N., Méndez-Blanco, C., Carbajo-Pescador, S., Fondevila, F., García-Palomo, A., González-Gallego, J., et al. (2017). Melatonin enhances sorafenib actions in human hepatocarcinoma cells by inhibiting mTORC1/p70S6K/HIF-1α and hypoxia-mediated mitophagy. *Oncotarget, 8*(53), 91402–91414.

Qi, M., Liu, C. Y., Zhao, Q., Zhang, Q. H., Hu, K. H., & Fu, J. S (2018). Polysaccharide antioxidant activities of *Panus giganteus*. *Mycosystema, 37*(12), 1707–1716.

Shi, F., Li, J. L., Ye, Z. Y., Yang, L. Q., Chen, T. T., Chen, X., et al. (2018). Antitumor effects of melanin from *Lachnum* YM226 and its derivative in H22 tumor-bearing mice. *MedChemComm, 9*(6), 1059–1068.

Shi, F., Li, J. L., Yang, L. Q., Hou, G. H., & Ye, M. (2018). Hypolipidemic effect and protection ability of liver-kidney functions of melanin from *Lachnum* YM226 in high-fat diet fed mice. *Food & Function, 9*(2), 880–889.

Song, S., Li, S. L., Su, N., Li, J. L., Shi, F., & Ye, M. (2016). Structural characterization, molecular modification and hepatoprotective effect of melanin from *Lachnum* YM226 on acute alcohol-induced liver injury in mice. *Food & Function, 7*(8), 3617–3627.

Sun, S. J., Zhang, X. J., Chen, W. X., Zhang, L. Y., & Zhu, H. (2016). Production of natural edible melanin by *Auricularia auricula* and its physicochemical properties. *Food Chemistry, 196*, 486–492.

Wang, Q., Wang, C. Y., Long, X. S., Wang, Z. C., & Ouyang, G. P. (2022). Research advances on synthesis and antitumor activity of 3-heterocyclic substituted indole derivatives. *Chemical Research and Application, 34*(09), 1955–1964.

Wang, Z. Y., Chang, M. Z., Xu, L. J., Meng, J. L., Zuo, N. K., & Pan, X. (2021). Structural characterization, physicochemical properties of melanin from fruiting body, hyphae and spores of *Ganoderma lucidum*. *Biotechnology Bulletin, 37*(11), 81–91.

Yang, L. Q. (2019). *Study of physicochemical properties and biological activity of melanin from Lachnum YM156*. Hefei University of Technology.

Yang, S. D., Bao, H. Y., & Wang, H. (2019). Chemical components and anti-tumour compounds from *Inonotus hispidus*. *Mycosystema, 38*(1), 127–133.

Yu, Z., Hu, W., Ma, K., et al. (2015). Physicochemical properties and antioxidant activities of melanin and fractions from *Auricularia auricula* fruiting bodies. *Food Science and Biotechnology, 24*(1), 15–21.

Zan, L. F., & Bao, H. Y. (2011). Progress in *Inonotus hispidus* research. *Acta Edulis Fungi, 18*(1), 78–82.

Zan, L. F., Liang, R. J., & Bao, H. Y. (2015). Antioxidant and antimicrobial activities of *Inonotus hispidus* extracts. *Northern Horticulture, 5*, 151–155.

Zhang, F. P., Xue, F. Z., Xu, H., Yuan, Y., Wu, X. P., Zhang, J. L., et al. (2021). Optimization of solid-state fermentation extraction of *Inonotus hispidus* fruiting body melanin. *Foods, 10*(12), 2893.

Zhang, M. R., Wang, Q. Q., Liu, T., & Guo, Z. (2016). Alkaline extraction optimization and characterization of *Auricularia auricula* melanin. *Food Science, 37*(12), 27–32.

Zhang, L. J., & Zhang, J. A. (2006). Study of extracting melanin from *Auricularia* and ITS stability. *Journal of Shandong Agricultural University (Natural Science Edition), 03*, 369–371.

Zhang, Y. L., Zhang, R. C., Zhang, R. M., Ai, M. Q., & Huang, F. (2011). Research progress of analysis methods of lignin structure. *Journal of Anhui Agricultural Sciences, 39*(36), 22514–22517.

Zhou, Y. Fermentative production of melanin by *Auricularia auricula* and its functional properties. Nanjing Agricultural University. (2011).

Zhu, C.P., Zhai, X.C., Zhang, X., Li, L.Q., Zhang, Q.A., Wu, X.X., & Deng, H. Research progress in extraction, separation, purification and bioactivity of *Pleurotus ostreatus* polysaccharides. *Science and Technology of Food Industry*, *36*(6) (2015), 359–364+369.